White Light Interferometry Utilizing the Large Measuring Volume of a Nanopositioning and Nanomeasuring Machine

D. Kapusi[1], T. Machleidt[1], E. Manske[1], K.-H. Franke[1,2], R. Jahn[2]
Technische Universität Ilmenau, Postbox 100 565, D-98684 Ilmenau, Germany;
ZBS Ilmenau e. V., Gustav-Kirchoffstr. 5, D-98693 Ilmenau, Germany;

mailto:daniel.kapusi@tu-ilmenau.de

Abstract: At the Technische Universität Ilmenau a nanopositioning and nanomeasuring machine (NPM machine) has been developed, which allows highly exact dimensional and traceable positioning with subnanometre resolution and nanometre uncertainty within a measuring volume of 25 x 25 x 5 mm^3. The article deals with the utilization of the device's very high precision and large effective range for white light interferometry. The height information is extracted from the measuring data by interferogram analysis with envelope and phase evaluation. Exemplary results of both classes of methods are compared. The capabilities of exact positioning enables the stitching of adjacent measurement areas without complex registration algorithms and independent of the sample topography. The resulting necessary calibration procedure and corrective actions are discussed. Furthermore, the scanning time for large steps in the vertical direction is decreased by defining multiple pass-through ranges. This allows the skipping of height ranges which are not of interest.

1. MOTIVATION

At the TU Ilmenau a nanopositioning and nanomeasuring machine (NPM machine) was developed under the leadership of the Institute of Process Measurement and Sensor Technology in cooperation with the Zentrum für Bild- und Signalverarbeitung Ilmenau e.V.[1] and the company SIOS Messtechnik GmbH[2]. The Collaborative Research Centre (SFB) 622 'Nanopositioning and Nanomeasuring Machines' supported by the German Research Foundation and the Thuringian Ministry of Education is now working on the basis of these developments.
The fundamental and innovative concept of the NPM machine is the realization of the Abbe comparator principle in all three measuring axes [Jäger 2001] – that means that the measuring probe and the measuring beams of the machine

[1] http://www.zbs-ilmenau.de
[2] http://www.sios.de

must be aligned. This has the effect of avoiding systematic and random tilting of the guide elements, also called first-order tilt errors.
The consequent observance of the principle has made possible a state-of-the-art nanopositioning and nanomeasuring machine with a resolution of 0.1 nm and a positioning repeatability below 0.3 nm within a measuring volume of 25 mm x 25 mm x 5 mm [Manske 2007]. In contrast to conventional coordinate measuring machines the sample is moved instead of the sensor. Sensors are fixed in such that their working point is located in the Abbe-point. The displacement of the sample can thus be measured with highest accuracy.
Besides the large effective range and the high resolution, a significant advantage of the device is that several different measuring methods can be applied. The different types of sensors are quickly and easily changeable because of their modular conception. So far atomic force microscopes, focus sensors as well as capacitive and inductive contact systems are applicable sensor types for the NPM machine. However, data capture for these sensors is limited to one dimension; the measuring data can only be acquired sequentially point by point. This also means that the measurement time requirements cannot ever be met. Parallel data collection is desirable, which is possible on the basis of white light interferometry, a powerful optical measuring method that allows the capturing of a whole surface with very high precision within a few seconds.
The integration of white light interferometry into the NPM machine is one of the current research and development topics of the Computer Graphics Group (TU Ilmenau). At this time a microscope tube with a magnification of nearly 0.5x is used. A Mirau interference objective with a magnification of 20.0x and a working distance of 4.7 mm is mounted on this tube. A halogen light source is coupled into the tube over a fiber optic cable. The measuring data are acquired by a 14-bit FireWire 1394b monochromatic CCD camera. The NPM machine is located on an oscillation damping system and is shielded from acoustic waves. Additionally, the acoustic enclosure is thermally stabilized.
White light interferometry can profit from the high positioning resolution and large measuring volume of the NPM machine. Hence, the main disturbing influence on the measurement accuracy, the positioning noise, can almost be completely avoided.
The capabilities of exact positioning enables the stitching of adjacent measurement areas without complex registration algorithms and independent of the topography of the sample to utilize the given large lateral effective area.
Furthermore, in contrast to modern conventional white light interferometers, whose perpendicularly pass-through ranges are limited in general to 100 µm, the combination with the NPM machine allows operating over a height range up to 5 mm. The measuring time can be accelerated significantly by skipping height ranges where no fringes occur, using a coarse speed during the perpendicular scan (see Figure 1).

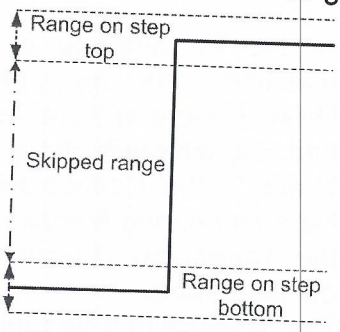

Figure 1; Skipping the z-scan range between the top and the bottom of a step

2. BASICS OF WHITE LIGHT INTERFEROMETRY

Several different basic types of interferometers can be used for micro-topographical measurements: Fizeau, Michelson, Mirau and Linnik. However, the fundamental principle is almost the same for all types.
The beam of a short coherent light source is split into two paths. Figure 2 shows the design of a Mirau interferometer, where the beam is split using a semi transparent mirror.
Along the first path (the reference path) the beam is reflected back by a reference mirror. Along the second path (the object path) the beam is reflected back by the surface of the sample.
The reflected beams of both paths are brought together again before they are captured by a camera. Fringes occur when the optical path difference between the reference and the object paths is lower than the coherence length of the light source. The fringes have maximum contrast when the optical path difference is zero. During the measurement the optical path difference is varied by moving the sample along the optical axis of the object path, so that whole fringes appear in each pixel of the camera. The interferograms are sampled by taking a picture with every pass of a constant step width.
To acquire height information for each pixel, the height position of the sample has to be recalculated, where the optical path difference was zero.

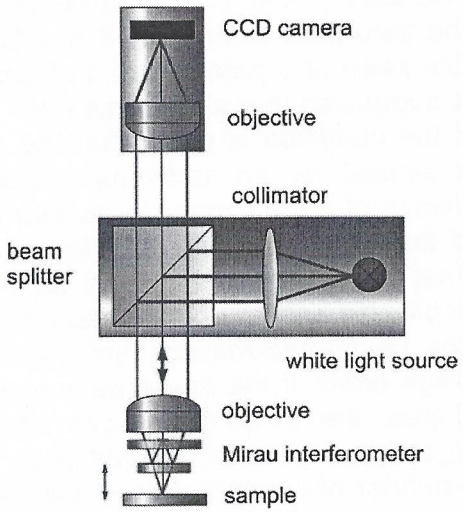

Figure 2; Design of a Mirau white light interferometer

3. INTERFEROGRAM ANALYSIS METHODS

The range of fringes is cut out of the captured images individually for each pixel position online during the measurement in a pre-processing step in order to reduce the amount of input data. This helps to save computing power and memory.
The interferograms are analyzed first by the envelope evaluation method. Besides the well-known methods for estimating the discrete envelope;

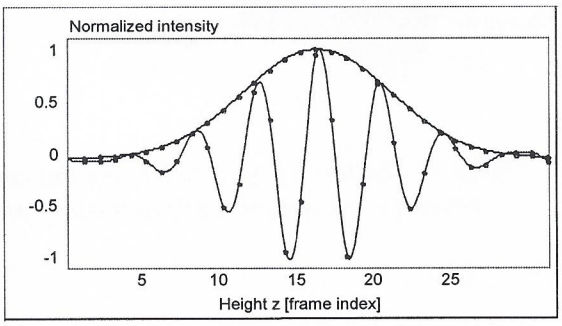

Figure 3; Interferogram sampled with a step width of 77 nm and its envelope

e.g. fast bucket methods or the Hilbert transformation; the slightly more CPU-intensive but also more robust approach of correlating the input interferogram with matched filters, performed in the frequency domain [Kapusi 2007], is favored.

The peak position of the envelope is coincident with the sought-after location of the zero path difference. It is estimated in the sub-frame range by means of a Gaussian or a parabola fit. In [Kapusi 2007] an iterative gradient-based method is suggested that also works well.

If the condition is given that the surface is smooth then the precision can be increased by an additional phase evaluation. The phase is determined by means of a Blackman-Harris [Harris 1978] windowed discrete Fourier transform at the interferogram's main frequency (twice the frequency of the light source). Fast bucket methods such as the Carré algorithm [Creath 1988] are also applicable but they provide less precision.

The height information from the envelope evaluation is used to determine the fringe order. If the envelope evaluation should be not applicable e. g. at strong slopes, the fringe order can alternatively be counted using an unwrapping algorithm. However, if height steps appear between adjacent pixels greater than a quarter of the light source wavelength, then the fringe order cannot be clearly determined. This limit can be extended in compliance with spatial constraints, assuming that the geometry of the sample is known a priori (e.g. a spherical form).

Three-dimensional visualization of the height data from section R1 [Koenders 2003] of a PTB layer thickness standard measured with a 77 nm step size in the z-direction and calculated by envelope and phase evaluation respectively are contrasted in Figure 4. The repeatability of determining the average step height in conformance with ISO 5436–1 has been estimated at over 30 single measurements of section R1 with a standard deviation of 0.51 nm for the envelope evaluation and 0.11 nm for the phase evaluation.

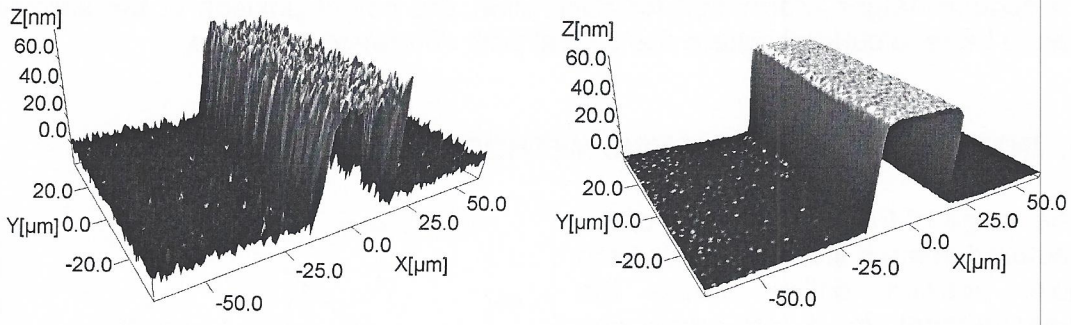

Figure 4; Section R1 of a PTB layer thickness standard SH70 analyzed once using envelope evaluation (left) and using phase evaluation (right) (dz = 77 nm)

4. STITCHING

Samples whose lateral extensions exceed the field of view (currently about 0.8 mm x 0.6 mm) are captured by stitching height maps from several single measurements at adjacent positions. Because of the capabilities of precision positioning, which tops the sub-pixel range many times over, the field of view can be exactly aligned for each measurement. This means that complex registration and resampling algorithms become unnecessary. This method even works if the topography of the sample is homogenous.

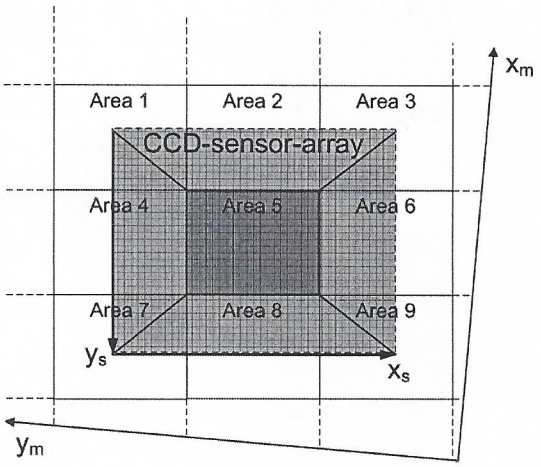

Figure 5; Array of fields of view aligned parallel to the axes of the sensor coordinate system

The partial height maps are then joined together into a large height map independent of the topography of the sample. This is done using the corresponding machine coordinates known to nanometer precision for each field of view to avoid error propagation from one single measurement area to the next.

In order to position the sample to achieve a regular grid of fields of view (as in Figure 5), the sensor must first be calibrated. The measuring head is assumed to be orthogonally aligned to the z-scan direction. The lateral relative transformation parameters (rotation, pixel spacing) from sensor (x_s, y_s) to machine coordinates (x_m, y_m) have to be determined.

4.1 Sensor Calibration

The idea of the calibration method is to register a list of pass points between two images of the same target object which have been captured at different lateral positions. An average translation vector is calculated over all corresponding point pairs. The relative transformation parameters can be calculated between the known translation vector of the machine coordinates and the translation vector between the pass points of the images.

A grid structure is used as a calibration target whose crossing points are treated as the points of interest. The gridlines are steadily detectable by means of the Hough transformation. The assignment of the pass points between the two images is done using the nearest neighbor principle, which assumes that the transformation parameters are roughly known beforehand. The calibration procedure has to be repeated until the average transformation parameters have reached the claimed uncertainty (e.g. 30 times to achieve an expanded positioning uncertainty of about U(k=2) = 0.05 pixel/mm).

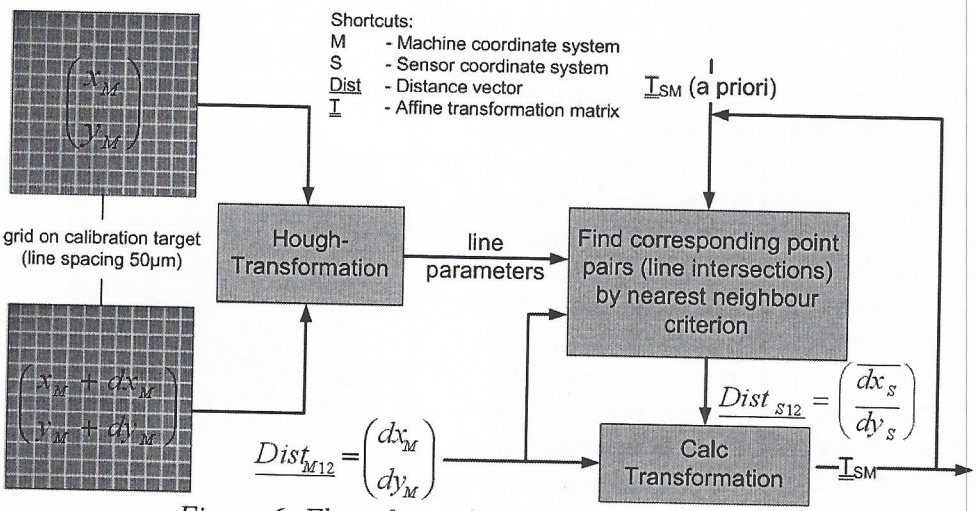

Figure 6; Flow chart of the calibration procedure

4.2 Treatment of the Sensor Tilt

The tilt of the sensor can be seen in the merged height data as jumps between the crossings of adjacent fields of view, if the tilt is not taken into account. It can be measured by calculating the height differences pointwise in the overlapping regions in the x- and y-directions. The influence of the sensor tilt in the height data can be excluded by calculating and adding the average difference plane sequentially to the height data of each field of view.

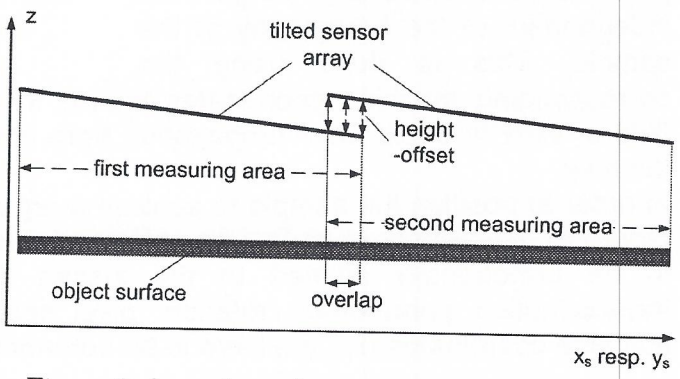

Figure 7; lateral overlap to determine the sensor tilt

5. DEVELOPMENT ENVIRONMENT

The control and analyzing software is realized within the VIP (Visual Image Processing) Toolkit[3] package developed by the ZBS (Zentrum für Bild und Signalverarbeitung) Ilmenau e.V., which is a cooperation partner of this project. The VIP toolkit already contains a huge number of image processing and control operators, which can be linked together within a graphical editor using pipelines. Furthermore, the toolkit can be extended by the implementation of individual operators. For each application it is also possible to develop a graphical user interface.

[3] http://www.zbs-ilmenau.de/html/prod/toolkit.html

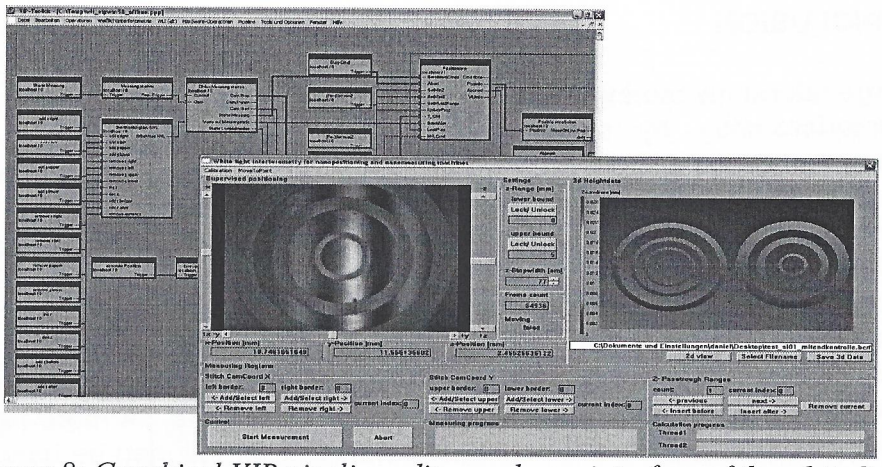

Figure 8; Graphical VIP pipeline editor and user interface of the white light interferometry application

6. EXEMPLARY RESULTS

The whole range of the PTB layer thickness standard SH70 was captured by stitching height data maps from 64 single measurements. The height data were calculated with phase evaluation of the measurement data, which were sampled with a z-scan step width of 77 nm. The whole measurement and data processing (@Intel®Core2 Duo 2x2667MHz) for the resulting measuring range of 4.16 mm x 4.05 mm took about 23 minutes. The stitched height data map contains more than 21 million data points with a spacing of 0.8 µm.

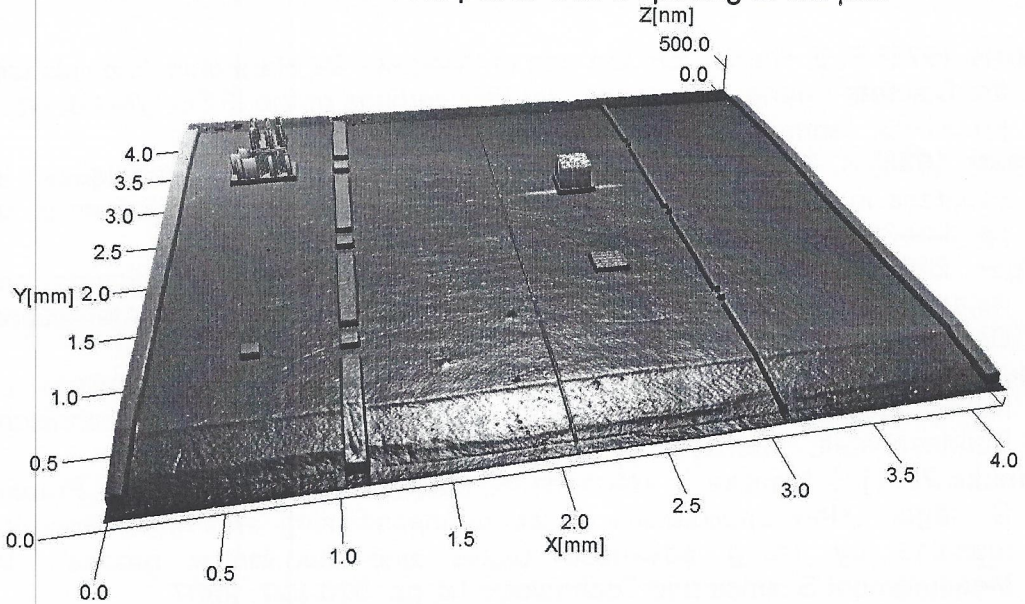

Figure 9; 3d visualization of a measured PTB layer thickness standard SH70 (stitching of 64 fields of view, more than 21 million data points)

7. CONCLUSION

The large lateral measuring range of the NPM machine can be utilized for white light interferometry by stitching the height data from several adjacent measurement areas without the loss of metrological accuracy and independent of the topography of the sample. The transformation parameters from the sensor to the machine coordinate system are detected by a calibration procedure in the run-up to the measurements. The large z-range is utilizable by skipping out-of-interest ranges and cutting out the interferogram range individually for each pixel during the perpendicular scan.
The next working steps will focus on the redesign of the measurement head, made of Invar, which will be slid into a Zerodur base plate. A more high-grade compact microscope tube with a magnification of 1.0x will then be used. The tilt of the sensor will be manually adjustable.

8. ACKNOWLEDGMENTS

The project white light interferometry for nanopositioning and nanomeasuring machines has been sponsored by the Thuringian Ministry of Education and the Arts (Germany) under the sign B 514-06 007. The authors wish to thank all those colleagues at the Technische Universität Ilmenau and the ZBS Ilmenau e.V. who have contributed to these developments.

9. REFERENCES

[Harris 1978] F. J. Harris; "On the use of Windows for Harmonic Analysis with the Discrete Fourier Transform"; *In:* Proceedings of the IEEE, Vol.66, No.1, pp. 51-83, January 1978

[Creath 1988] K. Creath; "Phase-Measurement Interferometry Techniques"; In: Progress In Optics Vol. XXVI, E. Wolf, Elsevier Science Publishers B. V., pp. 349-393; Amsterdam 1988

[Jäger 2001] G. Jäger, E. Manske, T. Hausotte; "Nanopositioning and measuring machine"; In: Proceedings of the 2nd euspen International Conference, Vol.1, pp. 290-293; Turin 2001

[Koenders 2003] L. Koenders; "WGDM-7: Preliminary Comparison on Nanometrology, Nano2: Step height standards"; Physikalisch Technische Bundesanstalt; Braunschweig 2003

[Manske 2007] E. Manske, T. Hausotte, R. Mastylo, T. Machleidt, K.-H. Franke, G. Jäger; „New applications of the nanopositioning and nanomeasuring machine by using advanced tactile and non-tactile probes"; In: Measurement Science and Technology 18, pp. 520-527; 2007

[Kapusi 2007] D. Kapusi, T. Machleidt, K.-H. Franke, R. Jahn; "White light interferometry in combination with a nanopositioning and nanomeasuring machine (NPMM)"; In: Proceedings of SPIE Vol. 6616, Munich 2007